The E22K mutation of myosin RLC that causes familial hypertrophic cardiomyopathy increases calcium sensitivity of force and ATPase in transgenic mice

Danuta Szczesna-Cordary*, Georgianna Guzman, Jiaju Zhao, Olga Hernandez, Jianqin Wei and Zoraida Diaz-Perez

Department of Molecular and Cellular Pharmacology, University of Miami School of Medicine, Miami, FL 33136, USA
*Author for correspondence (e-mail: dszczesna@med.miami.edu)

Accepted 13 May 2005
Journal of Cell Science 118, 3675-3683 Published by The Company of Biologists 2005
doi:10.1242/jcs.02492

Summary

Familial hypertrophic cardiomyopathy (FHC) is an autosomal dominant disease caused by mutations in all of the major sarcomeric proteins, including the ventricular myosin regulatory light-chain (RLC). The E22K-RLC mutation has been associated with a rare variant of cardiac hypertrophy defined by mid-left ventricular obstruction due to papillary muscle hypertrophy. This mutation was later found to cause ventricular and septal hypertrophy. We have generated transgenic (Tg) mouse lines of myc-WT (wild type) and myc-E22K mutant of human ventricular RLC and have examined the functional consequences of this FHC mutation in skinned cardiac-muscle preparations. In longitudinal sections of whole mouse hearts stained with hematoxylin and eosin, the E22K-mutant hearts of 13-month-old animals showed signs of inter-ventricular septal hypertrophy and enlarged papillary muscles with no filament disarray. Echo examination did not reveal evidence of cardiac hypertrophy in Tg-E22K mice compared to Tg-WT or Non-Tg hearts. Physiological studies utilizing skinned cardiac-muscle preparations showed an increase by $\Delta pCa_{50} \geqslant 0.1$ in Ca^{2+} sensitivity of myofibrillar ATPase activity and force development in Tg-E22K mice compared with Tg-WT or Non-Tg littermates. Our results suggest that E22K-linked FHC is mediated through Ca^{2+}-dependent events. The FHC-mediated structural perturbations in RLC that affect Ca^{2+} binding properties of the mutated myocardium are responsible for triggering the abnormal function of the heart that in turn might initiate a hypertrophic process and lead to heart failure.

Key words: Hypertrophic cardiomyopathy, Myosin regulatory light-chain, Muscles, Physiology

Introduction

Familial hypertrophic cardiomyopathy (FHC) is an autosomal dominant disease originating from mutations in genes that encode for the major proteins of the thick and thin filaments of cardiac muscle. Recent studies have revealed that the ventricular isoform of myosin regulatory light-chain [RLC; also known as myosin regulatory light-chain 2 (MLRV)] is one of the sarcomeric proteins associated with FHC (Andersen et al., 2001; Flavigny et al., 1998; Kabaeva et al., 2002; Poetter et al., 1996; Richard et al., 2003) (Z. T. Kabaeva, Genetic analysis in hypertrophic cardiomyopathy: missense mutations in the ventricular myosin regulatory light chain gene, PhD thesis, Humboldt Universitat zu Berlin, 2002). The clinical course of FHC is variable and ranges from benign to severe heart failure and sudden cardiac death. The patients can be asymptomatic; however, occurrences of shortness of breath, angina, palpitations and syncope may happen. FHC is the most common cause of sudden cardiac death in young adults, particularly in athletes (Maron et al., 1995; Maron et al., 2000). To date, ten RLC mutations identified in American, European and South African populations have been linked to FHC. Some of them (A13T, E22K and P95A) were shown to be associated with a particular subtype of FHC defined by mid-left ventricular obstruction (Poetter et al., 1996) whereas others (F18L, N47K, R58Q, K104E, D166V and Intron IVS5-2 and IVS6-1 splice site mutations) presented with a more classic form of FHC, which resulted in increased left ventricular wall thickness and abnormal ECG (Andersen et al., 2001; Flavigny et al., 1998; Kabaeva et al., 2002; Richard et al., 2003) (Z. T. Kabaeva, PhD thesis, 2002). The E22K mutation was one of the first RLC mutations associated with FHC and its phenotype showed massive hypertrophy of the cardiac papillary muscles and adjacent ventricular tissue (Poetter et al., 1996). In a later study of Kabaeva et al., the E22K mutation was associated with moderate septal hypertrophy, late onset of clinical manifestation, and benign disease course and prognosis (Kabaeva et al., 2002) (Z. T. Kabaeva, PhD thesis, 2002).

In this report, we have examined the physiological consequences of the E22K mutation in skinned papillary muscle fibers isolated from transgenic mice expressing the E22K mutation of human cardiac RLC. The current study is a continuation of our previous work where we showed that the bacterially expressed E22K mutant of human cardiac RLC had dramatically altered Ca^{2+} binding- and phosphorylation-properties compared with the wild type (WT) RLC (Szczesna et al., 2001). Specifically, we demonstrated that the E22K

mutation, which is localized in the proximity of the RLC phosphorylation site (Ser15) and its Ca^{2+} binding site (residues 37-48), prevented phosphorylation of RLC and decreased its affinity for Ca^{2+} by about 20-fold (Szczesna et al., 2001). Moreover, our recent study utilizing E22K-reconstituted skinned porcine muscle preparations showed a slight increase in the Ca^{2+} sensitivity of force and myofibrillar ATPase activity compared to WT-reconstituted preparations (Szczesna-Cordary et al., 2004). The current work supports our previous results and demonstrates that this E22K mutation when overexpressed in mouse cardiac muscle, increases Ca^{2+} sensitivity of myofibrillar ATPase activity and steady-state force by about $\Delta pCa_{50} \geqslant 0.1$. Previous and current results suggest that the FHC-associated perturbations of the RLC Ca^{2+} binding site that lead to alterations in the Ca^{2+}-dependent ATPase/force could be responsible for the E22K-linked pathogenesis of FHC. This supports our hypothesis that an intact Ca^{2+} binding site in RLC is important in the regulation of cardiac-muscle contraction in the normal and diseased state of the heart (Szczesna, 2003). Moreover, we have examined the gross morphology of the transgenic (Tg)-E22K hearts that seemed to recapitulate the human phenotype of FHC associated with this RLC-E22K mutation (Kabaeva et al., 2002; Poetter et al., 1996). Longitudinal sections of hematoxylin and eosin stained whole hearts of 13-month-old Tg-E22K animals showed enlarged inter-ventricular septa and papillary muscles compared with Tg-WT and/or Non-Tg littermates. However, no cardiac hypertrophy was found by echocardiography examination or judging by the heart weight to body weight ratios.

Materials and Methods

Generation of transgenic mice

All animal studies were conducted in accordance with institutional guidelines. We have generated transgenic mouse models for the myc-WT (wild type) and myc-E22K mutant of human cardiac RLC. The cDNAs of these two proteins were cloned into the unique *Sal*I site of the plasmid, α-myosin heavy-chain clone 26 (a generous gift from Jeffrey Robbins, Cincinnati Children's Hospital Medical Center, Cincinnati, OH). The resulting constructs contained about 5.5 kb of the mouse α-myosin heavy-chain promoter, including the first two exons and part of the third, followed by the myc-WT and/or myc-E22K cDNAs (534 bp), and a 630 bp 3′ untranslated region from the human growth hormone transcript. The N-terminal myc sequence (MEQKLISEEDLD) was necessary to distinguish between the endogenous (mouse) and the transgenic (human) RLC in all generated transgenic animals (designed by Todd Miller, University of Miami School of Medicine, Miami, FL). All of the founders were bred to non-transgenic B6SJL mice. Founders were bred several times until adequate numbers of F1 offspring were obtained for each line. Two lines of myc-WT and two of myc-E22K were utilized for histology and physiological studies.

Analysis of protein expression

About 10 mg of left ventricle tissue from transgenic myc-E22K, myc-WT and Non-Tg were minced in a solution of 1% SDS, 1% β-mercaptoethanol, 1 mM EDTA, 1 mM PMSF, 1 μl/ml protease inhibitor cocktail (Sigma), homogenized, clarified by centrifugation 18,000 ***g*** for 10 minutes and quantitated by Pierce Coomassie-Plus Assay (Fig. 1A). The extracts were loaded at 5-20 μg per lane and run on 15% SDS-PAGE for Coomassie staining, while about 0.5-10 μg per lane was run for western blotting. Alternatively, cardiac myofibrils (CMF) prepared from left and right ventricular walls, septa and papillary muscles of transgenic mice were used in protein quantitation assays. The transgenic protein was quantitated with polyclonal RLC CT-1 antibodies produced in this laboratory (raised against 15 residues from the C-terminus of human cardiac RLC). For standard western blots the secondary antibody was peroxidase-conjugated goat anti-rabbit IgG (Fig. 1A). We have also used fluorescent secondary antibodies that were conjugated with fluorescent dye Cy 5.5 to monitor transgenic and endogenous RLC (Fig. 1B). As shown in Fig. 1A, the transgenic myc-RLC (WT or E22K) migrates slower than the endogenous RLC due to the myc sequence attached to the WT protein. The percent transgenic protein was expressed as: transgenic myc-protein ÷ (endogenous protein + transgenic myc-protein) × 100. The transgenic protein was also visualized using monoclonal myc-antibodies (clone 9E10) raised to a peptide from the human MYC protein (sequence EQKLISEEDL) (Roche) (Fig. 1A). Quantitation of western blots was done using Scion

Fig. 1. Protein expression in transgenic mouse lines. Approximately 10 mg of left ventricle tissue from transgenic myc-E22K, line 2 (L2) and line 4 (L4), myc-WT, line 1 (L1) and line 2 (L2) as well as Non-Tg mice were processed (see Materials and Methods) and quantitated on 15% SDS-PAGE using either Coomassie gel staining or polyclonal RLC CT-1 antibodies produced in this laboratory (raised against 15 residues from the C-terminus of human cardiac RLC). (A) SDS-PAGE stained with Coomassie and western blots of Non-Tg, Tg-WT (L1 and L2) and Tg-E22K (L2 and L4) expressed in mouse left ventricular tissue. Cardiac myofibrils prepared from left and right ventricular walls, septa and papillary muscles of transgenic mice were loaded at 10-20 μg per lane, run on 15% SDS-PAGE for Coomassie staining, while approximately 0.1-10 μg of the left-ventricular (LV) muscle extracts were loaded per lane for western blotting. The blots were calibrated with purified recombinant myc-WT that showed a linear dependence in the range of 10-75 ng. The highest loading concentration of 75 ng is shown in the right lane of each blot. The endogenous RLC and transgenic myc-WT, and myc-E22K proteins were all quantitated using polyclonal RLC CT-1 antibodies. Note that transgenic myc-WT and myc-E22K proteins migrate slower than the endogenous RLC because of the myc sequence attached to their N-termini. This was true for the Coomassie-stained gel (left upper panel) and also for RLC-antibody-stained western blots (right panels). Alternatively, the amount of transgene expression was quantitated using monoclonal myc-antibodies (clone 9E10) raised to a peptide from the human MYC protein (left lower panel). (B) Visualization of western blots with fluorescence. Western blots treated with polyclonal RLC CT-1 antibodies were further processed with fluorescent secondary antibodies conjugated with fluorescent dye Cy 5.5. Like in Fig. 1A, myc-RLC migrates slower than endogenous RLC because of the additional myc sequence attached to the N-terminal region of Tg-E22K or Tg-WT proteins. Note that no background fluorescence was found in the blot, indicating that no nonspecific antibody binding or ectopic transgene expression occurred. (C) Multi-determination of transgenic protein expression. Coomassie-stained gels as well as standard and fluorescent western blots were quantitated. Percentages of protein expression were determined by using Coomassie staining (black bars), western blots 'standard' (gray bars) and western blots 'fluorescence' (striped bars) were as follows: Tg-WT L1, 8.9±5.0 (n=12), 11.9±5.2 (n=6) and 7.4±2.6 (n=8); Tg-WT L2, 24.5±3.8 (n=12), 29.2±8.8 (n=3) and 23.1±3.1 (n=9); Tg-E22K L2, 69.8±2.9 (n=12), 60.4±6.0 (n=6) and 65.4±7.1 (n=8) and Tg-E22K L4, 86.8±4.3 (n=12), 92.3±2.9 (n=12) and 80.7±3.0 (n=4), respectively. Data are expressed as the average of n measurements ± s.d.

Image Software (standard western blots recorded with UVP Imager) or the Odyssey Infrared Imaging System (LI-COR Inc., for fluorescent western blots and Coomassie stained gels) (Fig. 1C).

Histopathological characterization

After euthanasia, the hearts of 13-month-old mice from each group were excised and immersed in 10% buffered formalin. Slides of whole mouse hearts were prepared by American Histolabs, Inc. (Gaithersburg, MD). The paraffin-embedded longitudinal sections of whole mouse hearts stained with hematoxylin and eosin were examined for overall morphology, hypertrophy and myofilament disarray using a Leica DMIRB microscope and 40× 0.75 plan apochromat objective (Imaging Core Facility at University of Miami School of Medicine).

Echocardiography examination

Mice were anesthetized with a mixture of ketamine (42.8 mg/kg), xylazine (8.6 mg/kg) and acepromazine (1.4 mg/kg) by intraperitoneal injection. Echocardiography was performed using Toshiba PowerVision 7000 equipped with real-time digital acquisition (Toshiba Medical Systems) (Yang et al., 1999). M-mode measurements of left ventricular chamber dimensions in diastole (LVIDD) and in systole (LVIDS), inter-ventricular septum thickness in diastole (IVSTD) and in systole (IVSTS), and posterior wall thickness (LVPWS) were performed as described (Yang et al., 1999). Left ventricular shortening fraction (FS) was calculated from the formula: FS (in %) = [(LVIDD-LVIDS) ÷ LVIDD] × 100. The ejection fraction (EF) was calculated using the equation: EF (100%)=[(LVIDD)^3–(LVIDS)^3 ÷ (LVIDD)^3] × 100 (Yang et al., 1999).

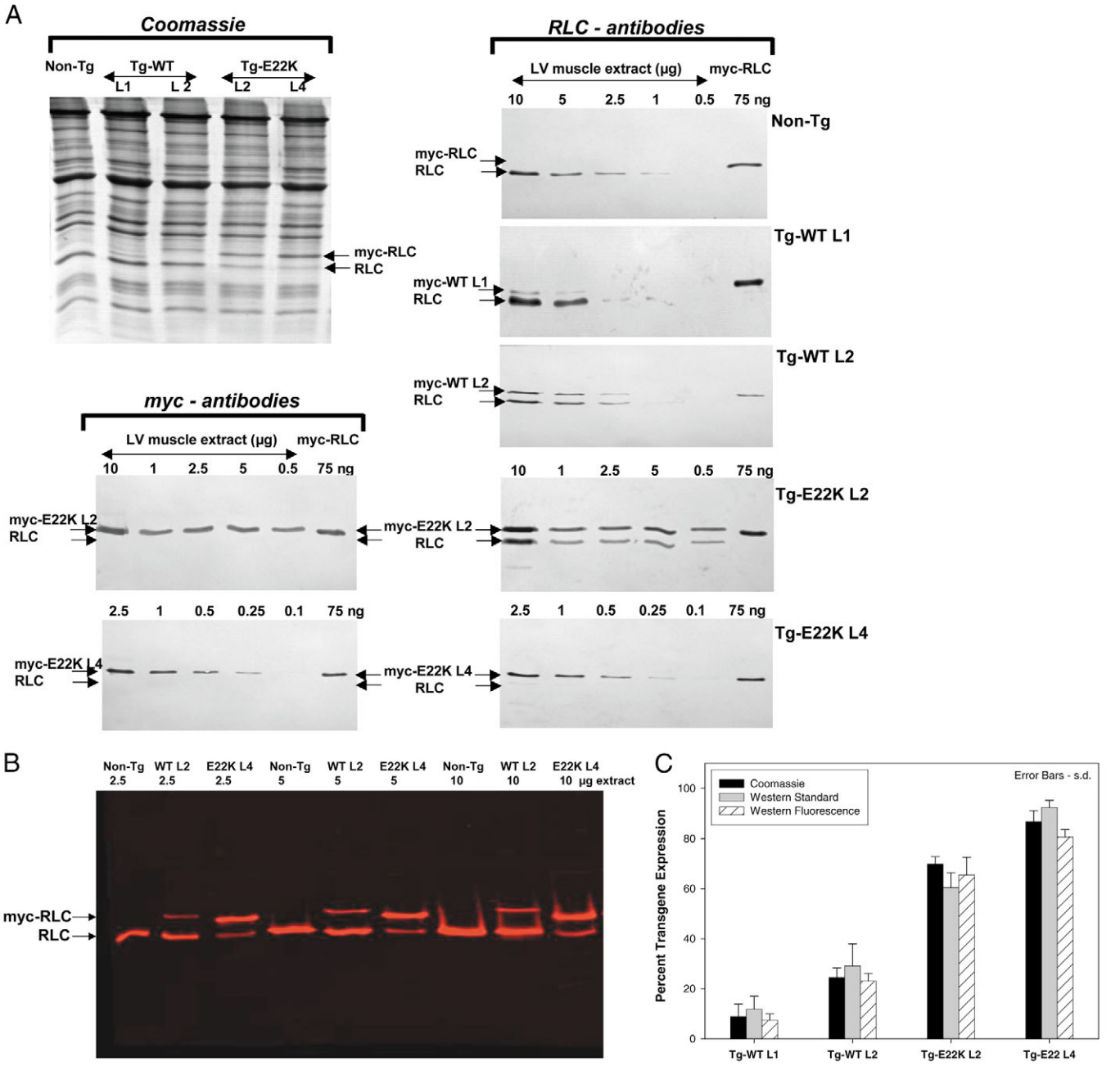

Fig. 1. See previous page for legend.

Myofibrillar ATPase activity

Cardiac myofibrils (CMF) were prepared from left and right ventricular walls, septa and papillary muscles of transgenic mice according to Solaro et al. (Solaro et al., 1971). Assays for myofibrillar ATPase activity of Non-Tg, Tg-WT and Tg-E22K CMF were performed in a solution of 20 mM MOPS pH 7.0, 40 mM KCl, 2.5 mM $MgCl_2$, 2 mM EGTA and increasing concentrations of Ca^{2+} from pCa 9 to pCa 4.5. After a 5-minute incubation at 30°C, the reaction was initiated with 2.5 mM ATP and terminated after 10 minutes with 5% trichloroacetic acid. Released inorganic phosphate was measured according to Fiske and Subbarow (Fiske and Subbarow, 1925).

Skinned fibers

Following euthanasia, hearts were quickly removed and rinsed free of blood in ice-cold saline (0.9% NaCl). Muscle strips 150-200 μm wide and 2-3 mm long were then quickly dissected from left ventricular papillary muscle, immersed in cold relaxing-solution and transferred into detergent-containing solution of 50% glycerol and 50% pCa 8 solution (10^{-8} M Ca^{2+}, 1 mM Mg^{2+}, 7 mM EGTA, 5 mM $MgATP^{2+}$, 20 mM imidazole, pH 7.0, 15 mM creatinine phosphate, ionic strength adjusted to 150 mM with KPr), containing 1% Triton X-100 for 24 hours at 4°C. Owing to the small size of these muscle strips they were not attached to support during glycerination. After a 24-hour skinning process with 1% Triton X-100, the fibers were transferred to the same glycerol containing solution without Triton X-100 and stored at –20°C until tested.

Steady-state force development

A bundle of approximately 3 to 5 fibers isolated from a batch of glycerinated mouse papillary fibers was attached by tweezer clips to a force transducer, placed in a 1 ml cuvette and bathed in pCa 8 solution. The fibers were then tested for steady-state force development in pCa 4 solution (composition is identical to pCa 8 solution except that the Ca^{2+} concentration is 10^{-4} M) and relaxed in pCa 8 solution. Steady-state force development was monitored for the control, Non-Tg fibers as well as for Tg-WT and Tg-E22K fibers.

Ca^{2+} dependence of force development

After the initial steady-state force was determined, the fibers were relaxed in pCa 8 solution and then exposed to solutions of increasing Ca^{2+} concentrations (from pCa 8 to pCa 4). The maximal force was measured in each "pCa" solution followed by a short relaxation of the fibers in pCa 8 solution. Data were analyzed using the following equations:

$$\%\ \text{force restored} = \frac{100 \times (\text{force restored} - \text{residual force})}{\text{initial force}}$$

and

$$\%\ \text{change in force} = \frac{100 \times [Ca^{2+}]^{n_H}}{[Ca^{2+}]^{n_H} + [Ca^{2+}{}_{50}]^{n_H}},$$

where $[Ca^{2+}{}_{50}]$ is the free Ca^{2+} concentration which produces 50% force and n_H is the Hill coefficient.

Rate of force activation and relaxation

For kinetic measurements the fibers were exposed to either DM-nitrophen or Diazo-2 to measure the rates of activation or relaxation, respectively, as described in Miller et al. (Miller et al., 2001).

Statistical analysis

Data are expressed as the average of n experiments ± s.e.m. (standard error of the mean). For experiments where only a few repetitions were available for the statistical analysis, the standard deviation (s.d.) was shown. The statistically significant difference between the pCa_{50} values in the Ca^{2+} sensitivity of myofibrillar ATPase activity and force development between the Tg-WT and the Tg-E22K mutant was determined utilizing an unpaired Student's t-test (Sigma Plot 8.0), with significance defined as $P<0.05$.

Results

Two transgenic mouse lines of myc-WT and two of myc-E22K were analyzed for protein expression, histopathology of the heart, echocardiography and for the Ca^{2+} sensitivity of ATPase activity and force development. The kinetics of force activation and relaxation were also measured. Physiological studies were assessed in skinned ventricular and papillary muscle preparations obtained from Non-Tg, Tg-WT and Tg-E22K mouse lines. About 10%, 25%, 65% and 87% of transgenic protein expression was determined for myc-WT-line 1 (L1), myc-WT-line 2 (L2), myc-E22K-line 2 (L2) and myc-E22K-line 4 (L4), respectively (Fig. 1). The percentage of Tg-protein expression was determined utilizing polyclonal RLC antibodies, which monitored the total RLC content (endogenous mouse and transgenic human myc-RLC). A monoclonal anti-myc-antibody (clone 9E10) raised to a peptide from the human MYC protein was used to confirm the identity of the transgenic human RLC construct. The amount of transgenic protein was visualized by SDS-PAGE, where a slower migration of the myc-RLC vs endogenous RLC was observed. This slower migration was due to the N-terminal myc sequence (MEQKLISEEDLD) of the transgenic protein (Fig. 1A,B). Fig. 1C summarizes transgenic protein expression determined by the band intensity analysis of Coomassie stained gels, standard western blots and western blots of the RLC labeled with fluorescent antibody. As shown, all three methods yielded similar results ± s.d. (Fig. 1C).

The gross heart morphology of Non-Tg, Tg-WT and and Tg-E22K mice is presented in Fig. 2A,B. Fig. 2A shows the longitudinal sections of the whole hearts from representative 13-month-old Non-Tg, Tg-E22K and Tg-WT animals. Fig. 2B shows higher magnification views of the respective heart slides shown in Fig. 2A. As indicated by arrows, enlarged inter-ventricular septa and papillary muscles (encircled) were observed in Tg-E22K mice compared with Tg-WT or Non-Tg littermates (Fig. 2A). The microscopic views of the ventricular and septal sections show no difference between the groups and no myofibrillar disarray was observed (Fig. 2B). Surprisingly, the echocardiography examination did not show any significant differences between the groups. The left ventricular chamber dimensions in systole and diastole, ejection or shortening fractions were relatively similar in all animals (Table 1). This result was in accord with the heart weight to body weight ratios (data not shown) that did not indicate cardiac hypertrophy in Tg-E22K vs control animals. Therefore, the human phenotype of septal and papillary muscles hypertrophy observed in patients harboring this mutation (Kabaeva et al., 2002; Poetter et al., 1996) could only be seen qualitatively in the slides of the whole hearts of Tg-E22K vs Tg-WT vs Non-Tg mice.

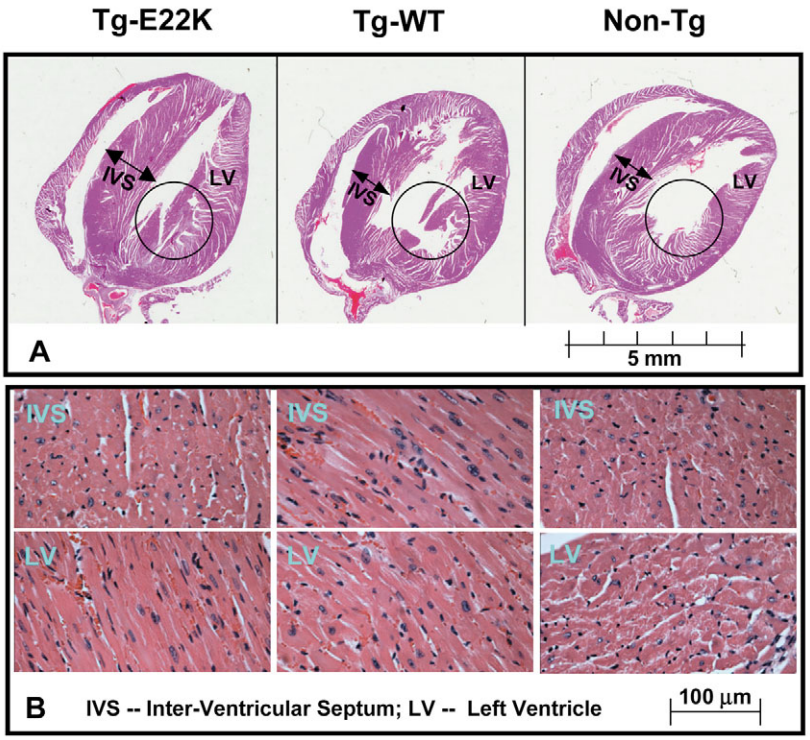

Fig. 2. Histology of transgenic mouse hearts. (A) Longitudinal sections of whole mouse hearts of Tg-E22K vs Tg-WT or Non-Tg mice. After euthanasia, the hearts of 13-month-old mice from Non-Tg, Tg-WT and Tg-E22K mice were excised and immersed in 10% buffered formalin. Longitudinal sections of the mouse hearts were stained with hematoxylin and eosin for overall morphology and hypertrophy. Note that the inter-ventricular septum (IVS) of Tg-E22K mice appears more massive than septa of Tg-WT or Non-Tg mice. Also, the papillary muscles of the left ventricles in Tg-E22K hearts appear more substantial than in Tg-WT or Non-Tg mice. (B) Microscopic views of the inter-ventricular septa (upper panels) and left ventricles (lower panels) of Tg-E22K vs Tg-WT or Non-Tg mouse hearts. As indicated, no myofilament disarray was observed in any presented heart tissue. Additionally there was no variation between different mouse lines. LVW, left ventricular wall; IVS, inter-ventricular septum.

Myofibrils from mouse ventricular, septal and papillary muscles of all groups were examined for their Ca^{2+} sensitivity of ATPase activity. In the control assays, transgenic wild-type (Tg-WT) mice expressing human isoform of RLC were compared to Non-Tg mice to test whether the Ca^{2+} sensitivity was RLC-isoform-dependent. As expected, the midpoints of Ca^{2+} sensitivity for these two curves were not different (Fig. 3) and pCa_{50}=6.27±0.04, n=7 (Tg-WT) vs pCa_{50}=6.23±0.03, n=10 (Non-Tg) (P>0.05). Statistically significant differences in the pCa_{50} values of the Ca^{2+} sensitivity of myofibrillar ATPase activity were observed between Non-Tg or Tg-WT and each line of mutant mice: Tg-E22K, line 2 (L2) (pCa_{50}=6.40±0.03, n=8) and line 4 (L4) (pCa_{50}=6.41±0.03, n=7) (P≤0.01). Both mutant lines increased the Ca^{2+} sensitivity of ATPase by about ΔpCa_{50}≅0.14 compared with Tg-WT myofibrils (P≤0.01) (Fig. 3B). Analogous effects of the E22K-dependent increase in Ca^{2+} sensitivity of force were observed in skinned papillary muscle fibers which, in addition, showed a slight gene dose effect. As demonstrated in Fig. 4, significant differences in the pCa_{50} values of the Ca^{2+} sensitivity of steady-state force were observed between Non-Tg (pCa_{50}=5.54±0.01, n=14) or Tg-WT (pCa_{50}=5.53±0.01, n=10) and each of the mutant lines, Tg-E22K, L2 (pCa_{50}=5.62±0.02, n=7) and L4 (pCa_{50}=5.65±0.01, n=12) (P≤0.001). Similar to the myofibrillar ATPase data, there was no difference in the midpoint of steady-state force-pCa dependence of Tg-WT and Non-Tg mice showing no variation in the force-pCa relationship between the murine and human isoforms of RLC. Interestingly, there was a slight gene-dose effect in the force development observed in the mutant fibers, i.e. between Tg-E22K, line 4 (87% transgene) and Tg-E22K, line 2 (65%) (Fig. 4A,B). The Ca^{2+} sensitivity of force in Tg-E22K L4 was slightly higher than in Tg-E22K L2 (pCa_{50}=5.65 vs 5.62) indicating a correlation between the increase in the pCa_{50} value with the increase of the transgenic protein expression level but the difference was not statistically significant (Fig. 4). The largest statistically significant increase in force development was caused by Tg-E22K L4, and compared with Tg-WT, the difference in ΔpCa_{50} was ≅0.12 (P<0.001). Moreover, the steepness (n_H) of the force-pCa dependences of the mutant fibers were lower than those of Non-Tg or Tg-WT fibers with the respective n_H values of 2.23±0.06, 2.44±0.08, 1.95±0.09 and 2.07±0.06 for Non-Tg, Tg-WT, Tg-E22K L2 and Tg-E22K L4 fibers (Fig. 4).

To assess the effect of the E22K mutation on the kinetics of force generating cross-bridges in skinned papillary muscle fibers, the activation- and relaxation-rates were examined with

Table 1. Echocardiography examination of Tg-E22K, Tg-WT and Non-Tg mice

	Tg-E22K n=5	Tg-WT n=4	Non-Tg n=4
LVIDD (mm)	3.28±0.04	3.10±0.16	3.20±0.08
LVIDS (mm)	1.64±0.13	1.57±0.15	1.55±0.10
IVSTD (mm)	0.66±0.05	0.65±0.05	0.65±0.05
IVSTS (mm)	1.24±0.05	1.22±0.05	1.20±0.00
LVPWD (mm)	0.66±0.05	0.60±0.00	0.62±0.05
LVPWS (mm)	1.26±0.05	1.22±0.05	1.22±0.05
FS (%)	49±4.3	50.3±2.1	51.2±2.9
EF (%)	85.6±3.2	86.5±1.9	87.5±2.4
HR (beats/min)	321±35	367±49	312±16

LVIDD and LVIDS, left ventricular inner diameter in diastole and systole; IVSTD and IVSTS, inter-ventricular septum thickness in diastole and in systole; LVPWD and LVPWS, LV posterior wall thickness in diastole and systole; FS, LV shortening fraction; EF, ejection fraction; HR, heart rate; see Materials and Methods for calculations (Yang et al., 1999). Data are mean± s.d.

DM-nitrophen or Diazo-2, respectively. Line 4 of Tg-E22K was utilized in these studies. The half time (in milliseconds) of Tg-E22K activation rate was 54.6±1.6 whereas that of Tg-WT was 54.2±1.9. The half times of relaxation measured in Tg-

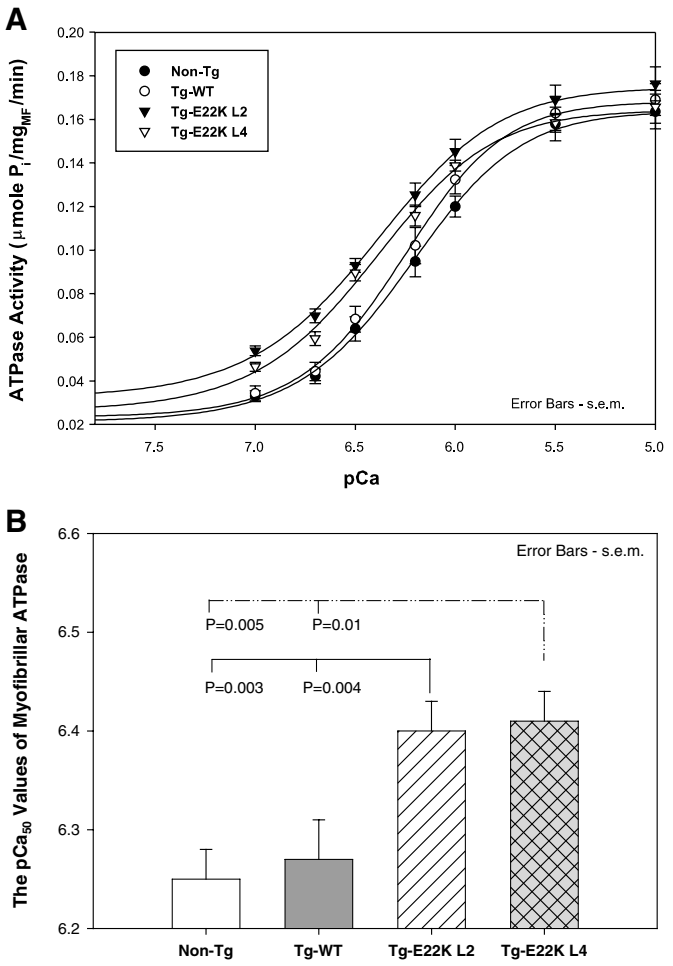

Fig. 3. Myofibrillar ATPase activity in transgenic cardiac-muscle preparations. Myofibrils from ventricular and papillary muscles from transgenic mice were examined for myofibrillar ATPase activity in a solution (see Materials and Methods) and increasing concentrations of Ca^{2+} (pCa 9 to pCa 4.5). After a 5-minute incubation period at 30°C, the reaction was initiated with 2.5 mM ATP and terminated after 10 minutes with 5% trichloroacetic acid. Released inorganic phosphate was measured according to Fiske and Subbarow (Fiske and Subbarow, 1925). (A) ATPase-pCa relationship for Non-Tg, Tg-WT, Tg-E22K L2 and Tg-E22K L4 mouse muscle myofibrils. Statistically significant differences in the pCa_{50} values of the Ca^{2+} sensitivity of myofibrillar ATPase activity were observed between Non-Tg (n=10) or Tg-WT (n=7) and two lines of the mutant mice, Tg-E22K, line 2 (L2) (n=8) and line 4 (L4) (n=7) ($P\leqslant0.01$). A difference of the ΔpCa_{50}=0.14 was observed between Tg-WT and Tg-E22K L4 myofibrils (P=0.01). Respective n_H values of the ATPase-pCa relationships were: 1.54±0.17, 1.67±0.20, 1.38±0.14 and 1.45±0.11 for Non-Tg, Tg-WT, Tg-E22K L2 and Tg-E22K L4 myofibrils. (B) The pCa_{50} values for the ATPase-pCa dependences of Non-Tg, Tg-WT, Tg-E22K L2 and Tg-E22K L4 mouse muscle myofibrils. The Ca^{2+} sensitivity in Tg-E22K L2 (pCa_{50}=6.40±0.03, n=8) and L4 (pCa_{50}=6.41±0.03, n=7) myofibrils was increased compared with Non-Tg (pCa_{50}=6.23±0.03, n=10) or Tg-WT (pCa_{50}=6.27±0.04, n=7) myofibrils. As indicated, the differences were statistically significant ($P\leqslant0.01$). Data are expressed as the average of n experiments ± s.e.m.

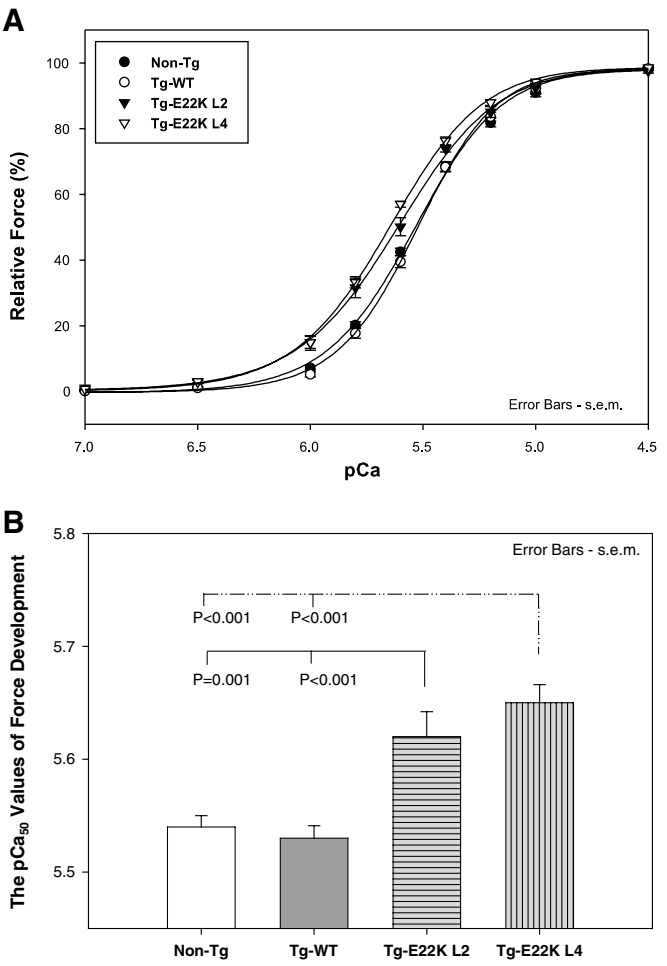

Fig. 4. Ca^{2+} sensitivity of steady-state force development in transgenic papillary muscle fibers. A bundle of approximately three to five fibers isolated from glycerinated mouse papillary muscle fibers was attached by tweezer clips to a force transducer and placed in a 1 ml cuvette. After the initial steady-state force was measured in pCa 4 solution, the fiber bundles were exposed to solutions of increasing Ca^{2+} concentrations (from pCa 8 to pCa 4). Measurements were performed for control, Non-Tg fibers as well as for Tg-WT, Tg-E22K L2 and Tg-E22K L 4 fibers. (A) The force-pCa relationship for Non-Tg, Tg-WT, Tg-E22K L2 and Tg-E22K L4 mouse papillary muscle fibers. Significant differences in the pCa_{50} values of the Ca^{2+} sensitivity of steady-state force were observed between Non-Tg (n=14) or Tg-WT (n=10) and two lines of Tg-E22K, line 2 (L2) (n=7) and line 4 (L4) (n=12) ($P\leqslant0.001$). The largest difference of the ΔpCa_{50}=0.12 was observed between Tg-WT and Tg-E22K L4 fibers (P<0.001). The steepness of the curves was lower for the mutant fibers and the respective n_H values were: 2.23±0.06, 2.44±0.08, 1.95±0.09 and 2.07±0.06 for Non-Tg, Tg-WT, Tg-E22K L2 and Tg-E22K L4 fibers. (B) The pCa_{50} values for the force-pCa relationships of Non-Tg, Tg-WT, Tg-E22K L2 and Tg-E22K L4 mouse papillary muscle fibers. The Ca^{2+} sensitivity in Tg-E22K L2 (pCa_{50}=5.62±0.02, n=7) and L4 (pCa_{50}=5.65±0.01, n=12) fibers was increased compared with Non-Tg (pCa_{50}=5.54±0.01, n=14) or Tg-WT (pCa_{50}=5.53±0.01, n=10) fibers. As indicated, the differences were statistically significant ($P\leqslant0.001$). Data are expressed as the average of n experiments ± s.e.m.

E22K fibers (64.6±3.9) were slightly higher than for Tg-WT (58.4±4.1) or Non-Tg fibers (57.6±1.1), however the difference was not significant ($P>0.05$).

In summary, although there was an increase in the Ca^{2+} sensitivity of force in E22K mutant skinned papillary muscle fibers, there was no difference in the kinetics of Ca^{2+}-dependent activation and Ca^{2+}-dependent relaxation in all examined transgenic lines.

Discussion

The gene for ventricular RLC (*MYL2*) has been mapped to chromosome 12q23-q24 (Macera et al., 1992; Seidman and Seidman, 1998) and expresses RLC in both, ventricular myocardium and slow-twitch muscle (Kubalak et al., 1994; Sarkar et al., 1971). The role of the ventricular isoform of RLC in cardiac-muscle contraction has been studied for some time and its importance in the physiological function of the heart is widely documented (for reviews, see Morano, 1999; Szczesna, 2003). In 1996 the ventricular RLC was first linked to FHC, and individuals identified with the E22K-RLC mutation experienced a rare phenotype of mid-ventricular cardiac obstruction due to massive papillary muscles and adjacent ventricular tissue hypertrophy (Poetter et al., 1996). A later study of Kabaeva and colleagues confirmed the left ventricular hypertrophy and showed in all E22K-affected individuals additional moderate septal hypertrophy, a late onset of clinical manifestation, and benign disease-course and -prognosis (Kabaeva et al., 2002) (Z. T. Kabaeva, PhD thesis, 2002). No cases of sudden cardiac death associated with this E22K mutation have been reported in any of these studies. The fact that the E22K mutation was found in various study populations (Kabaeva et al., 2002; Poetter et al., 1996) (Z. T. Kabaeva, PhD thesis, 2002) suggests that the codon 22 in exon 2 of the gene encoding RLC is highly susceptible to mutation.

To elucidate the mechanism by which the E22K mutation in RLC results in ventricular and/or septal hypertrophy and alters cardiac-muscle contraction in humans, we have generated transgenic mice overexpressing human cardiac E22K-RLC in murine heart. The expression of two lines of myc-WT and two lines of myc-E22K has been made under the control of the murine α-myosin heavy-chain promoter. The gross morphology of hematoxylin and eosin stained longitudinal sections of Tg-E22K mouse hearts demonstrated that their inter-ventricular septa as well as their papillary muscles were larger than those of Tg-WT or Non-Tg littermates. These experiments were performed utilizing hearts from 9-month-old mice (data not shown) and 13-month-old mice (Fig. 2). In both cases, the hearts of Tg-E22K mice demonstrated visibly enlarged inter-ventricular septa as well as papillary muscles (Fig. 2). These results suggested that the human phenotype of the E22K-mutated hearts (Kabaeva et al., 2002; Poetter et al., 1996) could be recapitulated in transgenic mice. As was shown by Kabaeva (Z. T. Kabaeva, PhD thesis, 2002), older individuals of a three-generation family carrying the mutation showed moderate hypertrophy of the entire septum, whereas younger patients had only mild or basal septal hypertrophy. Surprisingly, echocardiography abnormalities seen in most of the human patients with the E22K mutation have not been detected in our transgenic mice. The echocardiography examinations (Table 1) showed no significant differences in chamber dimensions in systole and diastole between Tg-E22K, Tg-WT and Non-Tg mice. The ejection and shortening fractions were also similar between the animals. At present, we have no obvious explanation why physiological differences between the mutant and the control lines as well as the different appearance in the histopathology images could not be supported by echocardiography results. Perhaps, more measurements and the use of newer echocardiogram technology developed for small animals could solve this discrepancy in the future. In vivo analysis of transgenic mice expressing the E22K mutation in the murine RLC isoform was recently reported by Sanbe and colleagues (Sanbe et al., 2000). Unlike the murine model carrying the human RLC gene-locus, mice with the mutated murine RLC cDNA failed to exhibit either overt hypertrophy or mid-ventricular cavity obstruction. Since the major focus of their study was the essential light-chain of myosin, no functional examination was performed or reported on their E22K-RLC transgenic mice (Sanbe et al., 2000).

The first investigated and reported transgenic animal models to study FHC-associated changes in the Ca^{2+} sensitivity of cardiac-muscle contraction were those expressing the thin filament regulatory proteins such as tropomyosin and troponin (James et al., 2000; Miller et al., 2001; Muthuchamy et al., 1999; Wolska et al., 1999). Our report presents similar Ca^{2+}-dependent alterations in contraction caused by a thick, and not thin, filament-containing protein, namely the myosin RLC. Moreover, this work is the first to investigate the functional consequences of the E22K mutation in human ventricular RLC in transgenic mice. Our findings that the E22K mutation increased Ca^{2+} sensitivity of myofibrillar ATPase activity and steady-state force development in transgenic skinned-cardiac-muscle preparations follow our earlier results in solution and in the reconstituted porcine fiber system. We showed that this mutation decreased Ca^{2+}-binding to isolated RLC (Szczesna et al., 2001) and slightly increased the Ca^{2+} sensitivity of force in the E22K-reconstituted porcine cardiac-muscle preparations (Szczesna et al., 2001). Our current studies with the E22K animal model support our earlier findings and therefore reveal the usefulness of transgenesis in the physiological characterization of the human disease in mice. Interestingly, the effect of the E22K-mediated increase in the Ca^{2+} sensitivity of force was shown by Levine and colleagues in biopsied slow skeletal muscle fibers from an E22K-diseased human patient (Levine et al., 1999; Levine et al., 1998). Consistently with our work, they showed an increase in the Ca^{2+} sensitivity of force development. Since the same gene expresses the ventricular- and slow-twitch skeletal muscle RLC (Kubalak et al., 1994; Sarkar et al., 1971), the comparison of their results from slow skeletal fibers with the ventricular fibers used in our work seems justified.

There are a few possible mechanisms for the E22K-mutated myocardium to initiate changes in the Ca^{2+} sensitivity of force/ATPase that could potentially trigger ventricular and/or septal hypertrophy as seen in human patients harboring this mutation. As a subunit of myosin, the RLC is known to stabilize the neck region of the myosin head, also called the lever-arm (Szczesna, 2003). This region of the myosin head has been postulated to undergo conformational changes that are important for the power stroke (Rayment et al., 1993a; Uyeda et al., 1996). As pictured in Fig. 5, the E22K mutation occurs

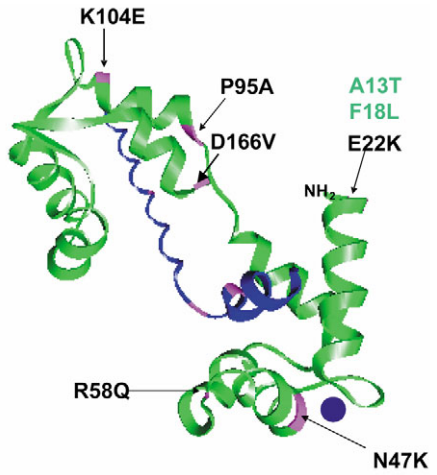

Fig. 5. Schematic representation of the regulatory light-chain of myosin (RLC) and the RLC-binding sequence of myosin heavy-chain. Sequences of the RLC and myosin heavy-chain were derived from the following crystal structures: NCBI numbers 1QVI and 1WDC (Gourinath et al., 2003; Houdusse et al., 1997). The FHC RLC one-point missense mutations are labeled. The A13T and F18L mutations are in the region of RLC that has not been solved in any of the existing crystal structures. The D166V mutation of RLC, the last identified to date, is incorrectly indicated as D166L in the original paper by Richard et al. (Richard et al., 2003) (revised information of P. Charron).

at the N-terminus of RLC, which is in close proximity to the C-terminal RLC-binding sequence of myosin heavy-chain in the head portion of myosin. This region in the crystal structure (NCBI numbers 1WDC and 1QVI) makes a sharp bend and connects the myosin head with the myosin rod (Gourinath et al., 2003; Houdusse et al., 1997; Rayment et al., 1993b). One can predict that any structural alterations in this pivotal region of myosin may affect the function of the lever arm and cause alterations in Ca^{2+}-dependent force generation in muscle. Lack of RLC phosphorylation caused by this E22K mutation, as shown by Szczesna and colleagues (Szczesna et al., 2001), could contribute to these myosin-dependent perturbations in force generation. However, the RLC is a member of the EF-hand Ca^{2+}-binding-protein family, like troponin C (TnC) and calmodulin. Ca^{2+}-binding to the RLC, like to other EF-hand Ca^{2+}-binding-proteins, could be a part of the Ca^{2+}-handling machinery in the muscle cell. The E22K mutation is localized in the helix preceding the Ca^{2+}-binding-loop of RLC and, as we have shown previously, replacement of the negatively charged glutamic acid with the positively charged lysine decreased binding of Ca^{2+} to RLC (K_{Ca}) 20-fold (Szczesna et al., 2001). One can speculate that, if binding of Ca^{2+} to the RLC plays a role in the overall Ca^{2+} homeostasis, this E22K amino acid change could directly interfere with this process because the RLC would no longer bind Ca^{2+} with the affinity of the wild-type protein. The observed increase in Ca^{2+} sensitivity of force/ATPase in Tg-E22K fibers could be a consequence of the E22K-mediated decrease in RLC Ca^{2+}-binding leading to an increase in overall Ca^{2+} concentrations that could be utilized by TnC, the key player of the Ca^{2+} regulation of muscle contraction. Similar cellular concentrations of both of these Ca^{2+} buffers, the RLC and the TnC, support this line of thinking. Another possibility is that the Ca^{2+} affinity and/or dissociation of TnC could be directly affected by this RLC mutation, leading to TnC-mediated Ca^{2+} alterations during contraction. Further experiments are needed to test the latter hypothesis. Interestingly, the kinetics of muscle contraction were not altered by this FHC RLC mutation and no significant changes in activation and relaxation rates among all three groups of animals were found. These results are in accord with in vitro motility assays by Poetter and colleagues, where the E22K-mutated myosin isolated from cardiac biopsies of affected individuals showed normal actin-filament translocation compared with control samples (Poetter et al., 1996).

In conclusion, our results suggest that E22K-mediated structural perturbations in the RLC-affecting Ca^{2+}-binding-properties of the mutated thick filaments are responsible for triggering the abnormal function of the filaments that in turn may initiate a hypertrophic process and lead to heart failure.

This work was supported by NIH-HL071778 and AHA Grant-In-Aid 0355384B (D.S.-C.).

References

Andersen, P. S., Havndrup, O., Bundgaard, H., Moolman-Smook, J. C., Larsen, L. A., Mogensen, J., Brink, P. A., Borglum, A. D., Corfield, V. A., Kjeldsen, K. et al. (2001). Myosin light chain mutations in familial hypertrophic cardiomyopathy: phenotypic presentation and frequency in Danish and South African populations. *J. Med. Genet.* **38**, E43.

Fiske, C. H. and Subbarow, Y. (1925). The colorimetric determination of phosphorus. *J. Biol. Chem.* **66**, 375-400.

Flavigny, J., Richard, P., Isnard, R., Carrier, L., Charron, P., Bonne, G., Forissier, J. F., Desnos, M., Dubourg, O., Komajda, M. et al. (1998). Identification of two novel mutations in the ventricular regulatory myosin light chain gene (MYL2) associated with familial and classical forms of hypertrophic cardiomyopathy. *J. Mol. Med.* **76**, 208-214.

Gourinath, S., Himmel, D. M., Brown, J. H., Reshetnikova, L., SzHent-Gyorgyi, A. G. and Cohen, C. (2003). Crystal structure of scallop Myosin S1 in the pre-power stroke state to 2.6 A resolution: flexibility and function in the head. *Structure* **11**, 1621-1627.

Houdusse, A., Love, M. L., Dominguez, R., Grabarek, Z. and Cohen, C. (1997). Structures of four Ca^{2+}-bound troponin C at 2.0 A resolution: further insights into the Ca^{2+}-switch in the calmodulin superfamily. *Structure* **5**, 1695-1711.

James, J., Zhang, Y., Osinska, H., Sanbe, A., Klevitsky, R., Hewett, T. and Robbins, J. (2000). Transgenic modelling of a cardiac troponin I mutation linked to familial hypertrophic cardiomyopathy. *Circ. Res.* **87**, 805-811.

Kabaeva, Z. T., Perrot, A., Wolter, B., Dietz, R., Cardim, N., Correia, J. M., Schulte, H. D., Aldashev, A. A., Mirrakhimov, M. M. and Osterziel, K. J. (2002). Systematic analysis of the regulatory and essential myosin light chain genes: genetic variants and mutations in hypertrophic cardiomyopathy. *Eur. J. Hum. Genet.* **10**, 741-748.

Kubalak, S. W., Miller-Hance, W. C., O'Brien, T. X., Dyson, E. and Chien, K. R. (1994). Chamber specification of atrial myosin light chain-2 expression precedes septation during murine cardiogenesis. *J. Biol. Chem.* **269**, 16961-16970.

Levine, R. J., Yang, Z., Epstein, N. D., Fananapazir, L., Stull, J. T. and Sweeney, H. L. (1998). Structural and functional responses of mammalian thick filaments to alterations in myosin regulatory light chains. *J. Struct. Biol.* **122**, 149-161.

Levine, R. J., Caulfield, J. B., Norton, P., Chantler, P. D., Deziel, M. R., Slayter, H. S. and Margossian, S. S. (1999). Myofibrillar protein structure and assembly during idiopathic dilated cardiomyopathy. *Mol. Cell. Biochem.* **195**, 1-10.

Macera, M. J., Szabo, P., Wadgaonkar, R., Siddiqui, M. A. and Verma, R. S. (1992). Localization of the gene coding for ventricular myosin regulatory light chain (MYL2) to human chromosome 12q23-q24.3. *Genomics* **13**, 829-831.

Maron, B. J., Gardin, J. M., Flack, J. M., Gidding, S. S., Kurosaki, T. T.

and Bild, D. E. (1995). Prevalence of hypertrophic cardiomyopathy in a general population of young adults. Echocardiographic analysis of 4111 subjects in the CARDIA Study. Coronary artery risk development in (young) adults. *Circulation* **92**, 785-789.

Maron, B. J., Olivotto, I., Spirito, P., Casey, S. A., Bellone, P., Gohman, T. E., Graham, K. J., Burton, D. A. and Cecchi, F. (2000). Epidemiology of hypertrophic cardiomyopathy-related death: revisited in a large non-referral-based patient population. *Circulation* **102**, 858-864.

Miller, T., Szczesna, D., Housmans, P. R., Zhao, J., deFreitas, F., Gomes, A. V., Culbreath, L., McCue, J., Wang, Y., Xu, Y. et al. (2001). Abnormal contractile function in transgenic mice expressing an FHC-Linked Troponin T (I79N) mutation. *J. Biol. Chem.* **276**, 3743-3755.

Morano, I. (1999). Tuning the human heart molecular motors by myosin light chains. *J. Mol. Med.* **77**, 544-555.

Muthuchamy, M., Pieples, K., Rethinasamy, P., Hoit, B., Grupp, I. L., Boivin, G. P., Wolska, B., Evans, C., Solaro, R. J. and Wieczorek, D. F. (1999). Mouse model of a familial hypertrophic cardiomyopathy mutation in alpha-tropomyosin manifests cardiac dysfunction. *Circ. Res.* **85**, 47-56.

Poetter, K., Jiang, H., Hassanzadeh, S., Master, S. R., Chang, A., Dalakas, M. C., Rayment, I., Sellers, J. R., Fananapazir, L. and Epstein, N. D. (1996). Mutations in either the essential or regulatory light chains of myosin are associated with a rare myopathy in human heart and skeletal muscle. *Nat. Genet.* **13**, 63-69.

Rayment, I., Holden, H. M., Whittaker, M., Yohn, C. B., Lorenz, M., Holmes, K. C. and Milligan, R. A. (1993a). Structure of the actin-myosin complex and its implications for muscle contraction. *Science* **261**, 58-65.

Rayment, I., Rypniewski, W. R., Schmidt-Base, K., Smith, R., Tomchick, D. R., Benning, M. M., Winkelmann, D. A., Wesenberg, G. and Holden, H. M. (1993b). Three-dimensional structure of myosin subfragment-1: a molecular motor. *Science* **261**, 50-58.

Richard, P., Charron, P., Carrier, L., Ledeuil, C., Cheav, T., Pichereau, C., Benaiche, A., Isnard, R., Dubourg, O., Burban, M. et al. (2003). Hypertrophic cardiomyopathy: distribution of disease genes, spectrum of mutations, and implications for a molecular diagnosis strategy. *Circulation* **107**, 2227-2232.

Sanbe, A., Nelson, D., Gulick, J., Setser, E., Osinska, H., Wang, X., Hewett, T. E., Klevitsky, R., Hayes, E., Warshaw, D. M. et al. (2000). In vivo analysis of an essential myosin light chain mutation linked to familial hypertrophic cardiomyopathy. *Circ. Res.* **87**, 296-302.

Sarkar, S., Sreter, F. A. and Gergely, J. (1971). Light chains of myosins from white, red, and cardiac muscles. *Proc. Natl. Acad. Sci. USA* **68**, 946-950.

Seidman, C. E. and Seidman, J. G. (1998). Molecular genetic studies of familial hypertrophic cardiomyopathy. *Basic Res. Cardiol.* **93**, 13-16.

Solaro, R. J., Pang, D. C. and Briggs, F. N. (1971). The purification of cardiac myofibrils with Triton X-100. *Biochim. Biophys. Acta* **245**, 259-262.

Szczesna, D. (2003). Regulatory light chains of striated muscle myosin. structure, function and malfunction. *Curr. Drug Targets* **3**, 187-197.

Szczesna, D., Ghosh, D., Li, Q., Gomes, A. V., Guzman, G., Arana, C., Zhi, G., Stull, J. T. and Potter, J. D. (2001). Familial hypertrophic cardiomyopathy mutations in the regulatory light chains of myosin affect their structure, Ca^{2+} binding, and phosphorylation. *J. Biol. Chem.* **276**, 7086-7092.

Szczesna-Cordary, D., Guzman, G., Ng, S. S. and Zhao, J. (2004). Familial hypertrophic cardiomyopathy-linked alterations in Ca^{2+} binding of human cardiac myosin regulatory light chain affect cardiac muscle contraction. *J. Biol. Chem.* **279**, 3535-3542.

Uyeda, T. Q., Abramson, P. D. and Spudich, J. A. (1996). The neck region of the myosin motor domain acts as a lever arm to generate movement. *Proc. Natl. Acad. Sci. USA* **93**, 4459-4464.

Wolska, B. M., Keller, R. S., Evans, C. C., Palmiter, K. A., Phillips, R. M., Muthuchamy, M., Oehlenschlager, J., Wieczorek, D. F., de Tombe, P. P. and Solaro, R. J. (1999). Correlation between myofilament response to Ca^{2+} and altered dynamics of contraction and relaxation in transgenic cardiac cells that express beta-tropomyosin. *Circ. Res.* **84**, 745-751.

Yang, X. P., Liu, Y. H., Rhaleb, N. E., Kurihara, N., Kim, H. E. and Carretero, O. A. (1999). Echocardiographic assessment of cardiac function in conscious and anesthetized mice. *Am. J. Physiol.* **277**, H1967-H1974.

Journal of Cell Science